Dynamic Mechanical Studies on Crystal Dispersion Using Ultradrawn Polyethylene Films

Masaru Matsuo,* Chie Sawatari, and Tomoko Ohhata

Department of Clothing Science, Faculty of Home Economics, Nara Women's University, Nara 630, Japan. *Received March 30, 1987*

ABSTRACT: The anisotropy of crystal dispersion was investigated by use of ultrahigh molecular weight polyethylene ($\bar{M}_v = 6 \times 10^6$) gel films which were prepared by gelation/crystallization from solution. The temperature dependence of the complex dynamic modulus was measured in the frequency range from 0.1 to 100 Hz, using undrawn and drawn gel films with various draw ratios up to 400. Superposition is realized by a combination of horizontal and vertical shifts resulting in apparent master curves of the storage and loss modulus functions. The Arrhenius plots of log shift factor versus the reciprocal of the absolute temperature indicates that there exist two mechanical dispersions corresponding to the α_1 and α_2 mechanisms, for drawn specimens whose draw ratios are lower than 100. The value of the activation energies associated with the α_1 and α_2 mechanisms for the undrawn gel and melt films are in the range of literature values which have been reported generally for semicrystalline spherulitic samples of high-density polyethylene with low molecular weights. The value associated with the α_1 mechanism decreases as a draw ratio increases but the value levels off when the draw ratio is beyond 100. The component of the α_2 mechanism decreases with increasing the draw ratio and becomes zero at a draw ratio of 400. Accordingly, it turns out that the α_2 mechanism cannot be observed when the external excitation is parallel to the crystal *c*-axis.

Introduction

It is well-known that dynamic mechanical analysis of polyethylene prior to melting reveals three peaks termed the α, β, and γ transitions.[1] The α and β transitions are commonly attributed to relaxation mechanisms in the crystal and amorphous phases, respectively, and the γ transition is due to the local motions of side groups associated with the amorphous fraction or defects in the crystalline phase.[2] Among the three transitions, the crystal dispersion (α transition) of polyethylene is reported to consist of two or more relaxation mechanisms. The resolution of the α transition into two components was first investigated by Nakayasu et al. for a melt-crystallized polyethylene.[3] They were designated as mechanisms I and II, with activation energies of the relaxation process of 117 and 201 kJ/mol, respectively. Since then, multiple types of crystalline relaxation mechanisms have been studied by various authors and mechanisms I and II have become known as α_1 and α_2, respectively.[4-6] Numerous studies on the α transition have indicated that the α_1 mechanism is associated with grain boundary phenomena concerning deformation and/or rotation of crystallites (crystal mosaic block) within a viscous medium and the α_2 mechanism with the crystal disordering transition due to the onset of torsional oscillation of polymer chains within the crystal lattice.[7-12] Takayanagi et al.[13,14] proposed that although the α_1 mechanism is complicated thermorheologically, the α_2 mechanism is simple, i.e., construction of master curves of the loss modulus requires only a horizontal shift of the isotherms along the frequency axis. From the relationship between the logarithm of the horizontal shift factor and the reciprocal absolute temperature, the activation energy of the α_2 mechanism of polyethylene was estimated to be 192 kJ/mol.

Stein et al.[15-19] and Kawai et al.[20-24] have shown that rheooptical studies may be used to investigate the nature of mechanical loss processes of semicrystalline polymers in connection with the deformation mechanism of the structural units. They have studied the deformation mechanism of semicrystalline polymers, e.g., spherulitic polyethylene films, by using dynamic X-ray diffraction and dynamic birefringence techniques. Kawai et al. concluded that the α_1 mechanism is due to grain boundary phenomena related to the morphology of the specimens.[21-24] These results were summarized by Kawai et al. in terms of the origin of the α_1 and α_2 mechanisms in high-density and low-density polyethylenes.[24]

According to their concept,[21-24] the α_1 mechanical dispersion is assigned to intralamellar grain boundary phenomena associated with reorientation of crystal grains within the orienting lamellae. The α_1 dispersion involves two types of preferential rotations of the crystal grains about their own crystal *a*- and *b*-axes, mostly at the polar and equatorial zones of the spherulites, respectively. On the other hand, the α_2 dispersion mechanism is assigned to an intracrystal lattice retardation phenomenon, observed by frequency dispersion of the complex dynamic compliance of the crystal lattice and may be ascribed to a smearing-out effect of the crystal lattice potential due to onset of rotational oscillations of polymer chains within the crystal grains.

In their studies,[15-24] however, it has been difficult to give an unambiguous interpretation of the relaxation mechanism because of the structural complexities of the semicrystalline spherulitic studies. Therefore, in order to further understand the origin of the α_1 and α_2 mechanisms, the present paper describes the crystal dispersion of polyethylene by a system that is morphologically simpler than a semicrystalline spherulitic one.

Undrawn and drawn polyethylene specimens produced by gelation/crystallization from dilute solutions have been used, since the morphological properties of the former specimen is similar to single crystal mats and the latter specimen is crystalline with the chains almost fully extended and aligned in the stretching direction.[25] For these specimens, the crystal dispersion was studied by measurements of the temperature–frequency dispersion of the complex dynamic tensile modulus.

Experimental Section

Sample Preparation. The sample used in this experiment was linear polyethylene (Hercules 1900/90189) with an intrinsic viscosity of 30 dL/g, corresponding to a viscosity-average molecular weight of 6×10^6. Gel films were prepared by the method proposed by Smith and Lemstra.[26,27] The gel films were stretched to desired draw ratios at 135 °C. Melt films were prepared from

* To whom all correspondence should be addressed.

0024-9297/88/2221-1317$01.50/0

Table I
Crystallinities and Melting Point of the Films[a]

specimens	crystallinity, %	mp, °C
melt film (λ = 1)	63	136.5
dry gel film (λ = 1)	85	140.0
dry gel film (λ = 20)	87	146.5
dry gel film (λ = 60)	90	150.5
dry gel film (λ = 100)	95	155.0
dry gel film (λ = 400)	98	155.0

[a] λ is a draw ratio.

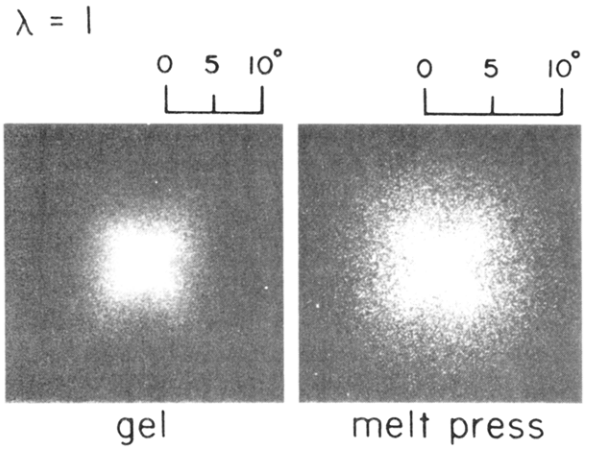

Figure 1. H_v light scattering patterns from the dry gel film and the melt film annealed for 1 h at 90 °C.

polyethylene powder to compare the mechanical dispersions with that of gel films. The powder was sandwiched between Teflon sheets at 200 °C for 10 min at a pressure of 1 GPa. The molten sample was cooled down to room temperature slowly.

Sample Characterization. The thermal behavior was estimated in terms of melting endotherms of differential scanning calorimetry (DSC) curves. Samples, weighting 5 mg, were placed in a standard aluminum sample pan. The samples were heated at a constant rate of 10 °C/min. The density of the films was measured in a pycnometer with chlorobenzene–toluene as a medium. Table I shows the results of crystallinities and melting points of drawn and undrawn films. As listed in Table I, the crystallinities and melting points of the gel film are higher than those of the melt film in an undeformed state and they increase with increasing draw ratio.

Light scattering patterns were obtained with a 3-mW He–Ne gas laser as a light source. Diffuse surfaces were avoided by sandwiching the specimen between microcover glasses with a silicon immersion oil having a similar index. Figure 1 shows H_v light scattering patterns from the undrawn melt and dry gel films which were annealed for 1 h at 90 °C. The intensity distribution has a maximum in the center and it decreases monotonically with increasing scattering angle. This observation is indicative of scattering from rodlike textures.

Small-angle X-ray scattering (SAXS) intensity distributions were detected with a position-sensitive proportional counter (PSPC) and a 12-kW rotating anode X-ray generator (Rigaku RDA-rA operated at 200 mA and 40 kV). Wide-angle X-ray diffraction (WAXD) patterns were obtained with a flat-film camera. These measurements have been discussed elsewhere.[28]

Figure 2 shows WAXD patterns of the dry gel and melt films annealed for 1 h at 90 °C. The patterns were obtained with the incident beam directed to the film surface. Figure 3 shows SAXS intensity distributions in the meridional direction with a PSPC. Curve a shows the profile from the melt film and curves b and c show profiles from an original dry gel film and annealed film. Annealing was done prior to measuring the dynamic mechanical properties of the samples. As illustrated in Figure 3, the intensity distribution of the melt film shows a monotonically decreasing curve. The distribution of the dry gel film shows the scattering maxima up to the fourth order but the maxima become indistinct with increasing annealing time. The periodic distances of the original gel and annealed gel films are 120 and 150 Å, respectively.

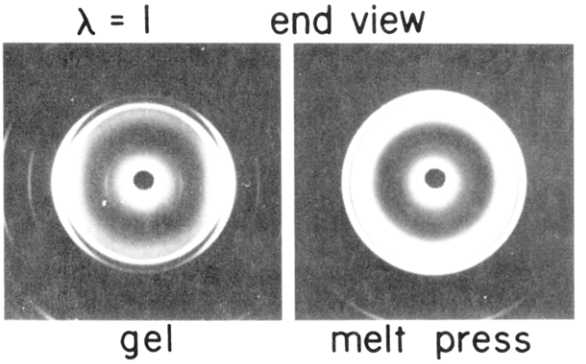

Figure 2. WAXD patterns from the dry gel film and the melt film annealed for 1 h at 90 °C.

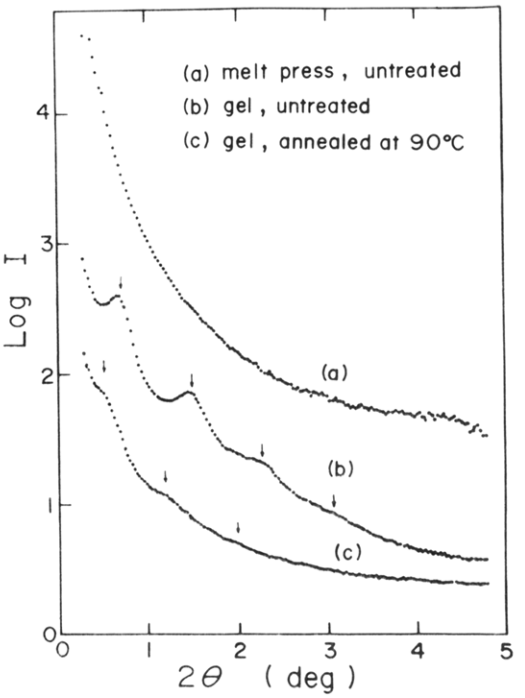

Figure 3. SAXS intensity distributions detected by PSPC: (a) the melt film; (b) the original dry gel film; (c) the dry gel film annealed for 1 h at 90 °C.

The results in Figures 2 and 3 indicate that crystal lamellae within the melt film are oriented randomly, while the dry gel film is composed of crystal lamellae that are highly oriented with their large flat faces parallel to the film surface. Within the lamellar crystals, the *c*-axes are oriented perpendicular to the large flat faces.

Experimental Procedure of the Viscoelastic Measurements. The complex dynamic tensile modulus functions were measured at frequencies from 0.1 to 100 Hz over the temperature range from 20 to 115 °C by using a viscoelastic spectrometer (VES-F) obtained from Iwamoto Machine Co., Ltd. The length of the specimen between the jaws was about 40 mm and the width was about 1.5 mm. During measurements, the film was subjected to a static tensile strain in order to place the sample in tension during the axial sinusoidal oscillation which had a peak deformation of 0.025%. The complex dynamic modulus was measured by imposing a small dynamic strain to assure linear viscoelastic behavior of the specimen. Before the measurements were made, the undrawn gel and melt films were annealed for 1 h at 90 °C and the drawn specimens were annealed for 1 h at the desired temperatures above 120 °C, as discussed later.

Results and Discussion

Figure 4 shows the temperature dependence of the storage modulus E' and the loss modulus E'' at a frequency of 10 Hz for the undrawn gel and melt films. It can be seen

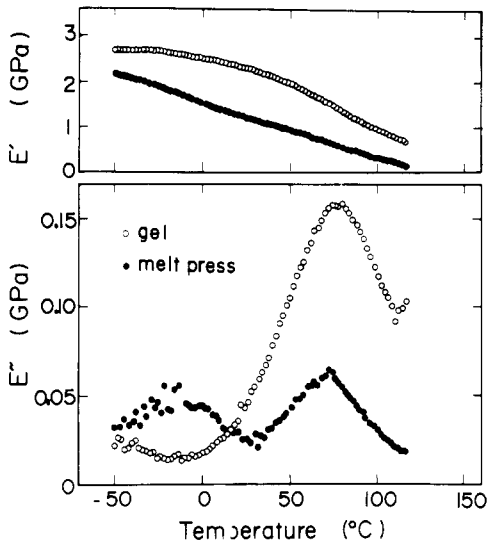

Figure 4. Temperature dependence of the storage modulus E' and the loss modulus E'' at a frequency of 10 Hz for the gel film and the melt film in an undeformed state.

that the storage modulus decreases with increasing temperature for both films. This tendency is similar to the results which have been observed by a number of authors for semicrystalline polymers with low molecular weights. The results indicate that the temperature dependence of E'' is affected by the crystallinity. The modulus of the gel film with high crystallinity (85%) has the α-transition and that of the melt film with low crystallinity (65%) has the β-transition around −20 °C in addition to the α-transition. This behavior is typical of polyethylene where single crystals do not exhibit the β-transition,[13,14] but where a small β-peak has been observed in bulk specimens.[23,24]

The α-peak of the gel film shows a large peak around 80 °C but that of the melt film shows a smaller peak around 72 °C. The peak temperature was discussed in relation to lamellar thickness by Khanna et al. for spherulitic specimens.[29] In this paper, however, the α-transition shall be analyzed in relation to crystallinity and crystal orientation in addition to lamellar thickness.

In order to carry out such a detailed analysis of the α-transition, the temperature dependence of E' and E'' was measured as a function of frequency. Figure 5 shows the result of the gel film. Profile a shows the behavior of E' between 10 and 115 °C, while curves b and c show those of E'' from 10 to 65 °C and from 70 to 90 °C, respectively. It can be seen that all the storage modulus functions decrease with increasing temperature at a given frequency, as well as with decreasing frequency at a fixed temperature. The loss modulus E'' is represented in the two ranges of temperatures from 10 to 65 °C and from 70 to 90 °C in order to facilitate discussion of the mechanical dispersion. According to viscoelastic theory, it may be expected that the loss modulus should show, at least, one dispersion peak. The loss modulus apparently shows only a broad continuous dispersion over the given frequency range. It is also noteworthy that above 90 °C the E'' data exhibit unusual behavior in that the increase in the magnitude of E'' with decreasing frequency becomes abruptly more pronounced in the range below 5 Hz. This behavior, however, is not shown in this paper. This is probably due to greater contribution to E'' from mechanism III reported by Nakayasu et al.[3] This is in accordance with the fact that dispersions found at lower frequencies have greater apparent activation energies. These unusual trends pose problems in constructing master curves by frequency–temperature superposition. Hence in order to carry out

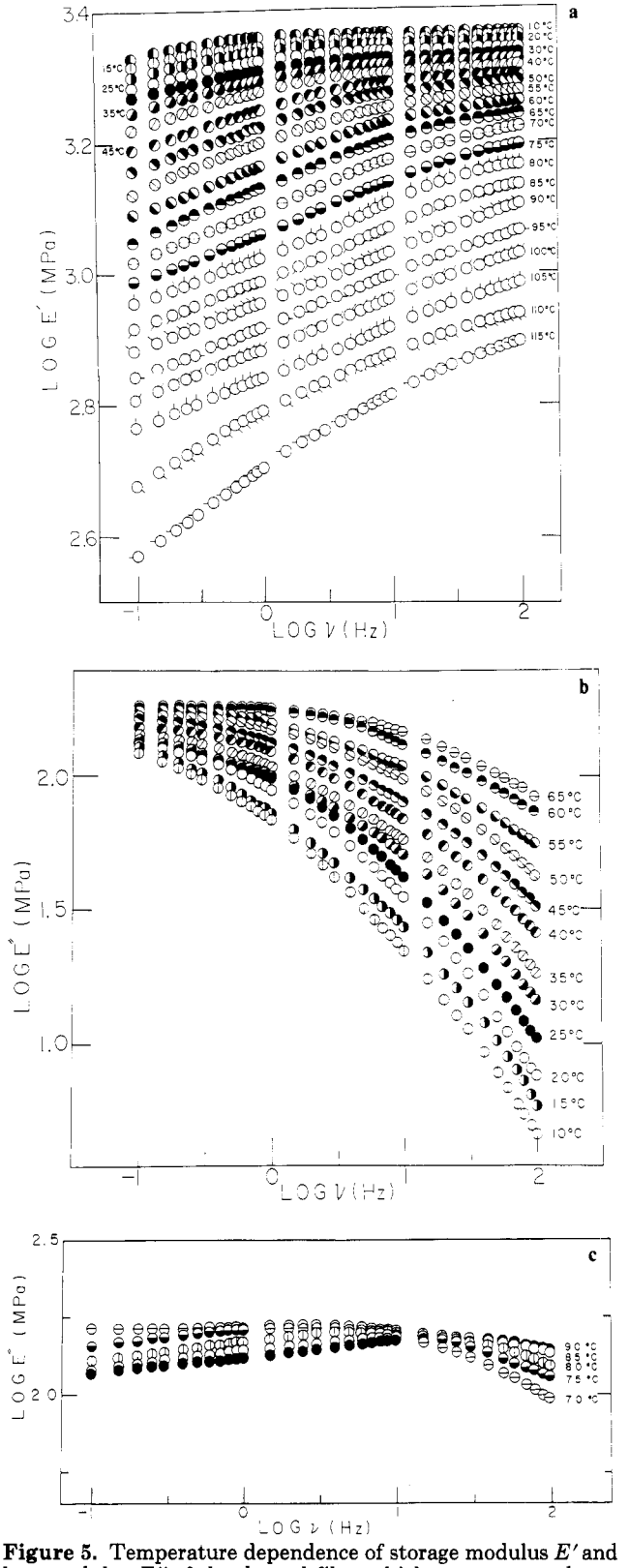

Figure 5. Temperature dependence of storage modulus E' and loss modulus E'' of the dry gel film, which was measured as a function of frequency: (a) the storage modulus E' measured in the temperature range from 10 to 115 °C; (b) the loss modulus E'' from 10 to 65 °C; (c) the loss modulus E'' from 70 to 90 °C.

the superpositions, it was necessary to eliminate all E'' data pertaining to temperatures in excess of 90 °C.

Figure 6 shows the master curves of E' and E'' for the dry gel film, reduced to the common reference temperature of 65 °C. Each curve is obtained by shifting horizontally and then vertically until good superposition is achieved. It is seen that the frequency dispersion of E'' exhibits a

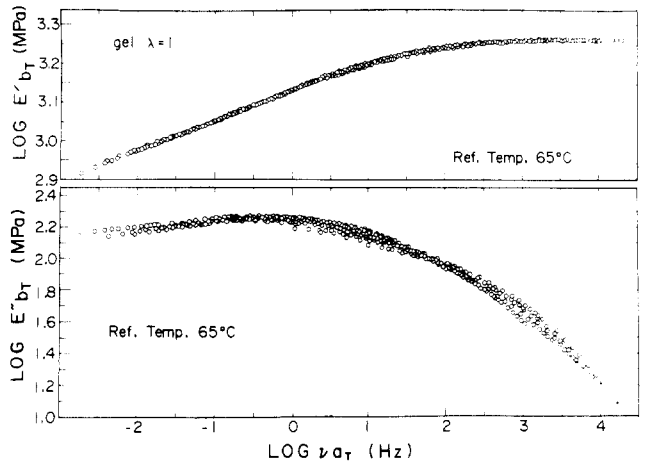

Figure 6. Master curves of the storage modulus E' and loss modulus E'' for the dry gel film.

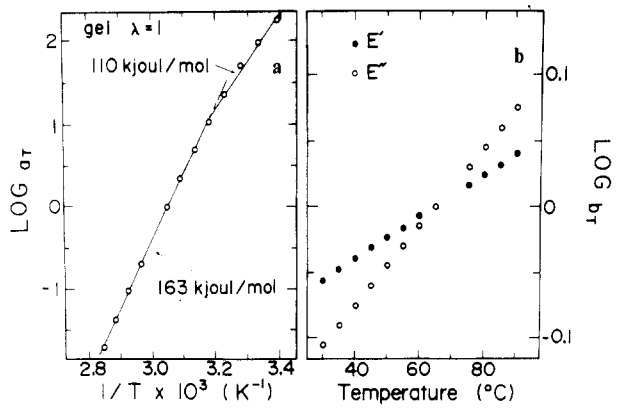

Figure 7. (a) Arrhenius plots of the horizontal shift factor $a_T(T,T_0)$ and (b) the logarithm of the vertical shift factor $b_T(T,T_0)$ versus temperature for the dry gel film.

quite broad dispersion peak and the profile is not symmetrical with respect to the logarithmic frequency axis. From these observations it can be inferred that although the broad dispersion curves may be expected to consist of two mechanisms, the direct separation of the reduced modulus into the respective contributions cannot be carried out owing to the lack of adequate data, especially in the lower frequency range. In order to classify the broad dispersion curve into two components, the logarithm of the temperature dependence of the horizontal shift factor $a_T(T,T_0)$ was plotted against reciprocal absolute temperature as shown in Figure 7a. The Arrhenius plots thus obtained are represented by two straight lines above and below the reference temperature of 65 °C. The activation energies obtained from the slopes of these lines are given as 110 and 163 kJ/mol, respectively, as indicated in this figure. These results clearly indicate that the broad dispersion curve consists of two components. Denoting the low and high-temperature mechanisms as α_1 and α_2, respectively, as has been done in numerous previous studies, it turns out that the estimated values of the activation energies are in the two ranges of the literature values of high-density polyethylene, i.e., from 98[24] to 117 kJ/mol[3] for α_1 and 147[24] to 193 kJ/mol[13,14] for α_2.

Here it should be noted that vertical shift is significant in construction of the master curves. Figure 7b shows the temperature dependence of the vertical shift factors $b_T(T,T_0)$ of E' and E''. As can be seen in the figure, the temperature dependence of $b_T(T,T_0)$ is given by a common straight line when plotted in logarithmic terms against a linear scale of temperature.

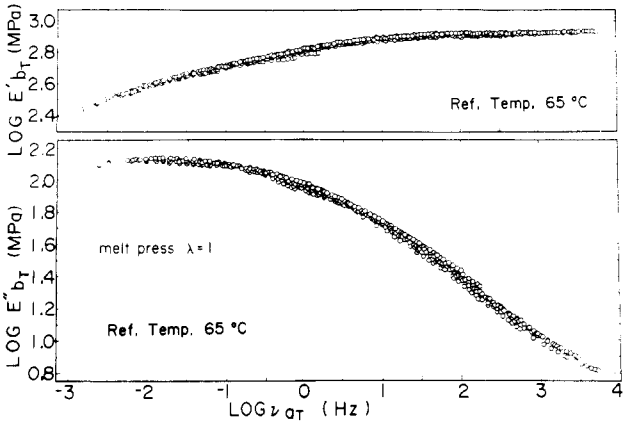

Figure 8. Master curves of the storage modulus E' and the loss modulus E'' for the melt film.

According to Takayanagi et al.,[13,14] the temperature–frequency superposition of polyethylene single-crystal mats required only a horizontal shift along the logarithmic frequency axis, and the activation energy was evaluated as 192 kJ/mol, associated with the α_2 mechanism. Thus, they concluded that such a simple superposition phenomenon for the α_2 mechanism is due to the dispersion with a single coefficient of internal friction, which uniquely determines the temperature dependence of the relaxation time associated with all of the vibrational modes of motion. Here it should be noted that in Takayanagi's paper, the contribution of the α_1 mechanism to the crystal dispersion of the single-crystal mats was not reported. However, the master curves of E' and E'' for the dry gel film can be formed by a vertical shift. The two kinds of activation energies indicate the existence of the α_1 and α_2 mechanisms, even though the constituent lamellar crystals within the gel film become oriented parallel to the film surface in a manner similar to single-crystal mats.[30-33] This discrepancy is probably due to the fact that the crystal lamellae within the dry gel film have a number of crystal defects and therefore are less ordered than single crystals produced with low molecular weight polyethylene. If the α_1 mechanism is associated with intercrystal-mosaic-block relaxation within the lamellae as reported by Suehiro et al.,[23] the imperfections in crystal lamellae within the dry gel film cause the α_1 mechanism.

In order to justify the significance of the vertical shift in constructing the master curves of E' and E'', we shall briefly summarize some references. The significance of the vertical shift factor was discussed in terms of Nagamatsu's[34] and Miki's approaches.[35,36] The former approach is based on the temperature dependence of amorphous entropic elasticity supplemented by the volume effect of the amorphous regions, while the latter approach takes into account the temperature dependence of crystal elasticity, based on a theory by Wada[37] and Okano,[38] of a smearing-out effect on the intermolecular potential within a crystal lattice. However, Suehiro et al.[23] reported that both of the approaches give a much smaller temperature dependence of the vertical shift factor than that required for fitting the experimental data. They pointed out that the shift factor is related to the temperature dependence of the crystal elasticity in the polar zone within polyethylene spherulites on the basis of the temperature dependence of the structural and mechanical parameters of the spherulitic model. Accordingly, the vertical shift for the α_2 mechanism shown in Figure 7b can be explained well by the concept of Suehiro et al.[23] but is in contradiction with that by Takayanagi et al.[13,14] Here it is evident that if the concept by Suehiro et al. is correct, the mechanical

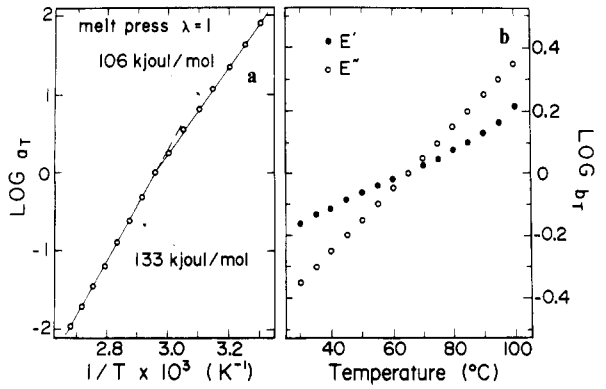

Figure 9. (a) Arrhenius plots of the horizontal shift factor $a_T(T,T_0)$ and (b) the logarithm of the vertical shift factor $b_T(T,T_0)$ versus temperature for the melt film.

behavior of crystallites perpendicular to the chain axis is certainly due to the temperature dependence of crystal elasticity, since the crystal lattice modulus in the chain direction is independent of temperatures below the normal melting point (145.5 °C).[39]

Figure 8 shows the master curves of E' and E'' for the undrawn melt film whose crystal orientation is random. The curves could be obtained by shifting horizontally and then vertically. The profile of E'' shows a broad dispersion similar to that of the dry gel film shown in Figure 6.

In order to obtain the activation energies, the logarithm of the temperature dependence of the horizontal shift factor $a_T(T,T_0)$ was plotted against reciprocal absolute temperature as shown in Figure 9a. The activation energies are given as 106 and 133 kJ/mol. The former obviously corresponds to the α_1 mechanism and the latter the α_2 mechanism. These values are similar to those obtained for a medium-density polyethylene (Sumitomo test polymer KP 119, Sumitomo Chemical Co.) and a high-density polyethylene (Monsanto test polymer MPE 200, Monsanto Co.).[24] Comparing the values in Figure 9a with those in Figure 7a, the value of the α_1 mechanism for the gel film is higher than that for the melt film. This result may be rigorous on the basis of two experimental results which have been reported by a number of authors: (1) The value of the activation energy for the α_2 mechanism for single-crystal mats is higher than that for spherulitic specimens.[13,14,24] (2) Among spherulitic specimens, both the values of the α_1 and α_2 mechanisms become higher as the crystallinity increases. The former result is probably related to molecular orientation in addition to crystallinity and the latter only to crystallinity.

In order to check the above concept, the temperature dependences of E' and E'' were measured as a function of frequency for the gel films with draw ratios of λ = 20, 60, and 100. The master curves were constructed by using these results. Prior to the measurements, all the specimens were annealed for 1 h at 120 °C. Figures 10 and 11 show the master curves of E' and E'', respectively, which could be obtained by shifting horizontally and then vertically. The master curves of E' show that the frequency dependence becomes smaller with increasing draw ratio, while those of E'' show a broad dispersion. This is similar to the results of the dry gel film and the melt film shown in Figures 6 and 8, respectively.

Figure 12 shows Arrhenius plots of the horizontal shift $a_T(T,T_0)$ used to obtain activation energies and shows the vertical shift $b_T(T,T_0)$ versus temperature. As indicated in this figure, the activation energy for the α_2 process decreases with increasing draw ratio. Furthermore, the vertical shifts of E' and E'' increase linearly with the same

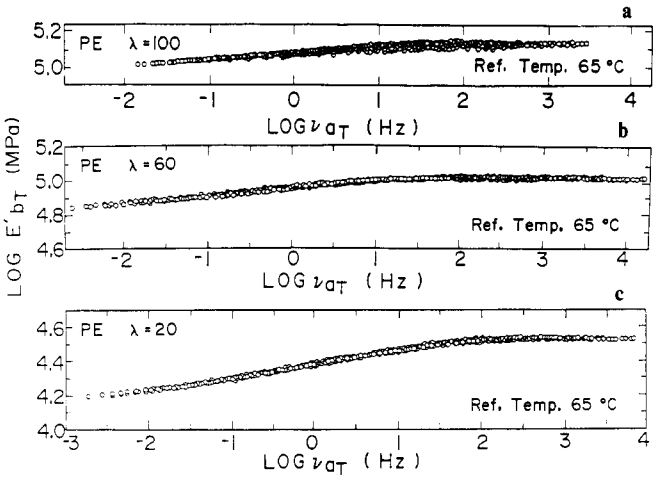

Figure 10. Master curves of the storage modulus E' for the dry gel films with (a) λ = 100, (b) λ = 60, and (c) λ = 20.

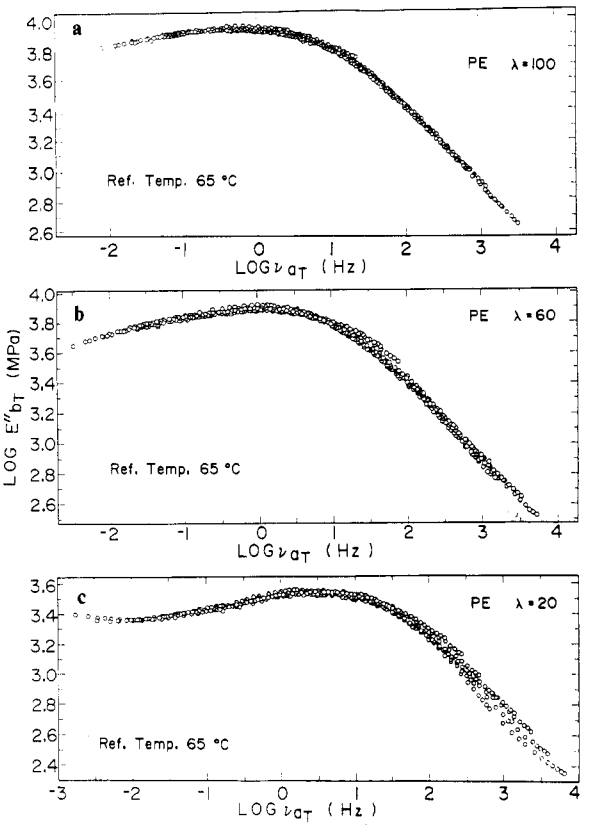

Figure 11. Master curves of the loss modulus E'' for the dry gel films with (a) λ = 100, (b) λ = 60, and (c) λ = 20.

value, and the increasing ratio becomes lower as the draw ratio increases. Such a tendency becomes more pronounced for an ultradrawn film with λ = 400.

Figure 13 shows the master curves of E' and E'' for the ultradrawn film (λ = 400) annealed for 1 h at 130 °C, prior to the measurements. The profile of E' shows that the frequency dependence is significantly smaller than that of other specimens. The value of E'' decreases considerably with increasing frequency beyond 10 Hz. This tendency indicates that this specimen with λ = 400 behaves like elastic materials. The storage modulus at 20 °C was 216 GPa in the frequency range beyond 10 Hz, which corresponds to Young's modulus of hard steel. The master curve of E'' shows a sharper dispersion than those of the other specimens as shown in Figures 6, 8, and 10. However, it can be inferred that direct separation of the reduced modulus into the respective contributions cannot be car-

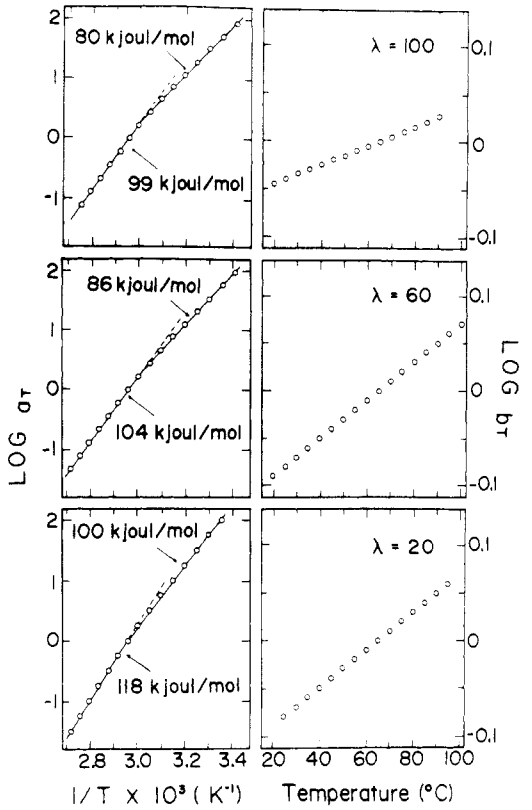

Figure 12. Arrhenius plots of the horizontal shift factors $a_T(T,T_0)$ and the logarithm of the vertical shift factors $b_T(T,T_0)$ versus temperature for the dry gel films with λ = 100, 60, and 20.

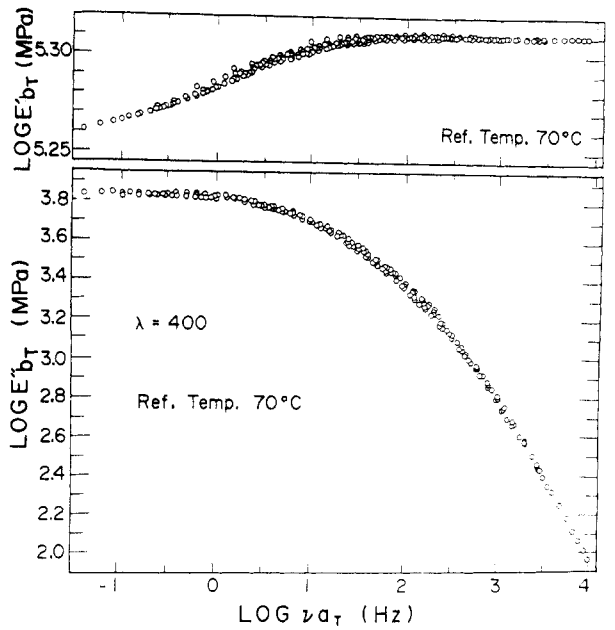

Figure 13. Master curves of the storage modulus E' and the loss modulus E'' for the dry gel film with λ = 400.

ried out as discussed before.

Figure 14a shows the Arrhenius plots of the horizontal shift factor $a_T(T,T_0)$, and Figure 14b shows the logarithm of the vertical shift factor $b_T(T,T_0)$ versus temperature. The Arrhenius plots are represented as a straight line. This result indicates that there exists only one mechanical dispersion whose activation energy is 79 kJ/mol. Here it should be noted that the superposition of E'' required only a horizontal shift along the logarithmic frequency axis and that of E' required a very small vertical shift in addition to the horizontal one. As discussed before, Takayanagi pointed out that the temperature–frequency superposition associated with the α_2 mechanism required only a horizontal shift but the superposition associated with the α_1 mechanism can be realized by horizontal and vertical shifts.[13,14] The question can be asked whether his concept proposed on the basis of the results for single crystal mats is applicable to the systems with greater molecular orientations.

In order to propose a general concept of crystal dispersion of polyethylene, we refer to the concept of Suehiro et al. which was derived from rheooptical studies.[22-24] They pointed out that the α_2 mechanism depends upon the temperature dependence of the crystal modlus of crystallites in the horizontal direction within spherulites. This indicates that the contribution of the α_2 mechanism is significant when the crystal c-axes are oriented perpendicular to the external applied excitation. In contrast, the α_2 mechanism does not appear for the ultradrawn film with λ = 400, and the dispersion with an activation energy of 79 kJ/mol corresponds to the α_1 mechanism, since the second-order orientation factor of this specimen was almost unity, denoting the perfect orientation of crystallites.[40]

Table II summarizes the change in activation energies of the α_1 and α_2 mechanisms with draw ratio. We shall use these results in referring to the α_1 and α_2 mechanisms. Among the specimens, the activation energies of the gel film are higher than those of the melt film. The dispersion strength of the α_2 mechanism becomes smaller with increasing draw ratio λ and finally becomes zero at λ = 400. Thus, only the α_1 mechanism was observed in the indicated temperature range. As discussed before, it was inferred that the α_2 mechanism is obviously observed when the external applied excitation is perpendicular to the c-axis but is less obvious when the applied excitation is parallel to the c-axis. Therefore, if the α_2 dispersion is ascribed to the smearing-out effect of the crystal lattice potential due to onset of rotational oscillation of polymer chains within the crystal grain as pointed out by Kawai et al.,[24] the smearing-out effect must be most active when the direction of the external applied stress is perpendicular to the crystal c-axis. This concept reasonably explains the experimental results. For example, Figures 2 and 3 show that the crystal c-axes within the undrawn gel film take a preferential orientation perpendicular to the direction of applied stress and that those within the melt film take a random orientation. Thus, it may be concluded that the α_2 mechanism is related to the anisotropy of crystallites.

The activation energy of the α_1 mechanism decreases with increasing draw ratio but it tends to level off beyond λ = 100, indicating a draw ratio which reflects a limiting high orientation of the c-axes.[40] This result indicates that the α_1 mechanism must be treated in relation to the relative orientation of polymer chains as is the case with the α_2 mechanism. If the α_1 mechanism for a spherulitic specimen is assigned to interlamellar grain boundary phenomena associated with reorientation of crystal grains due to their own preferential rotation within the orienting crystal lamellae, it may be expected that the α_1 mechanism of the ultradrawn film with λ = 400 is related to the slippage of crystal grains in the direction of the c-axis, when the external excitation is parallel to the c-axis, since rotation of the crystallites cannot occur in ultradrawn films. Furthermore if the morpholigical properties of grain boundaries are correlated with the activation energy, the value of the energy associated with the shear deformation parallel to the crystal c-axis should be different from that associated with the deformation perpendicular to the c-axis. Thus, it may be concluded that the activation energy

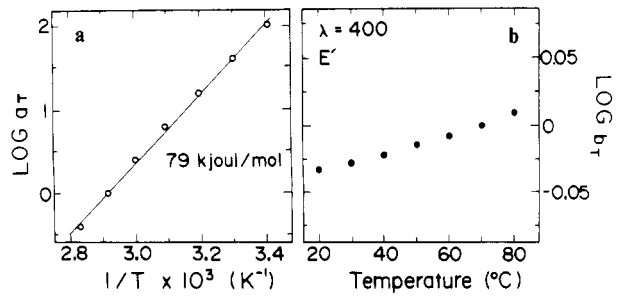

Figure 14. (a) Arrhenius plot of the horizontal shift factor $a_T(T,T_0)$ and (b) the logarithm of the vertical shift factor $b_T(T,T_0)$ versus temperature for the dry gel film with λ = 400.

Table II
Activation Energies of the α_1 and α_2 Mechanisms of the Films[a]

specimens	activation energies, kJ/mol	
	α_1 mechanism	α_2 mechanism
melt film (λ = 1)	106	133
dry gel film (λ = 1)	110	163
dry gel film (λ = 20)	100	118
dry gel film (λ = 60)	86	104
dry gel film (λ = 100)	80	99
dry gel film (λ = 400)	79	

[a] λ is a draw ratio.

of the α_1 mechanism decreases with increasing draw ratio. For ultradrawn film (λ = 400) with perfect orientation of the c-axes the temperature–frequency superposition does not require a vertical shift. This is due to the fact that the crystal lattice modulus in the direction of the c-axis is independent of temperatures below 145 °C and the thermal expansion coefficient was very small.[40]

Conclusion

The crystal dispersion (α dispersion) of polyethylene has been studied in terms of crystal orientation in the direction of external applied excitation. Three kinds of specimens were used. One was an undrawn gel film whose constituent lamellar crystals were oriented parallel to the film surface in a manner similar to mats of single crystals. The second was an undrawn melt film whose crystal orientation is random. The third was the drawn gel films whose draw ratios were in the range 20–400. The temperature dependence of the complex dynamic tensile modulus was measured in the range of frequency from 0.1 to 100 Hz for all the specimens. The master curves were constructed by shifting horizontally and then vertically. The Arrhenius plots, except for the specimen with a maximum draw ratio of 400, could be represented by two straight lines indicating the existence of two kinds of relaxation process. Thus, it was confirmed that the low- and high-temperature relaxations correspond to the α_1 and α_2 mechanisms, respectively. The activation energies as well as the vertical shift factor for both mechanisms became lower with increasing draw ratio. Thus, it turned out that the α_2 mechanism is obviously observed when the external applied excitation is perpendicular to the c-axis but is less obvious when the external excitation is parallel to the c-axis. Actually, the α_2 mechanism cannot be observed for the ultradrawn film (with a draw ratio of 400) having a near perfect crystal orientation of the c-axes with respect to the stretching direction where the Arrhenius plots were represented as a straight line. The α_1 mechanism observed for undrawn films generally is assigned to intralamellar grain boundary phenomena associated with the rotation of crystal grains in the direction of external excitation. This rotational behavior corresponds to the slippage of the grains in the c-axis direction for ultradrawn films. If the frictional coefficient between the grains along the c-axis is much lower than that associated with the rotation, the observed energy of the relaxation process for ultradrawn films is substantially lower than the values generally observed for normal samples. The vertical shift used in constructing the master curves of the ultradrawn film (λ = 400) was zero for the loss modulus and was very small for the storage modulus. This it is thought to be due to the fact that although the vertical shift is related to the temperature-dependence of the crystal elasticity, the crystal lattice modulus in the chain direction is independent of temperatures below 145 °C.

Acknowledgment. We thank Dr. Suehiro, Department of Polymer Chemistry, Faculty of Engineering, Kyoto University, for valuable comments and suggestions on preparing this paper.

Registry No. Polyethylene, 9002-88-4.

References and Notes

(1) Raff, R. A. V. In *Encyclopedia of Polymer Science and Technology*; Mark, H. F., et al., Eds.; Wiley: New York, 1967; Vol. 6, pp 275–332.
(2) Hoffman, J. D.; Williams, G.; Passaglia, E. *J. Polym. Sci., Part C* **1966**, *14*, 173.
(3) Nakayasu, H.; Markovitz, H.; Plazek, D. J. *Trans. Soc. Rheol.* **1961**, *5*, 261.
(4) Takayanagi, M.; Matsuo, M. *J. Macromol. Sci., Phys.* **1967**, *B1*, 407.
(5) Saito, N.; Okano, K.; Iwayanagi, S.; Hideshima, M. In *Solid State Physics*; Ehrenreich, H., Seitz, F., Turnbull, D., Eds.; Academic: New York, 1963; Vol. 14, p 458.
(6) Iwayanagi, S., paper presented at the 2nd Kyoto Seminar on Polymers, Kyoto, 1968.
(7) Tsuge, K.; Enjoji, H.; Terada, H.; Ozawa, Y.; Wada, Y. *Jpn. J. Appl. Phys.* **1962**, *1*, 270.
(8) Iwayanagi, S.; Miura, I. *Jpn. J. Appl. Phys.* **1965**, *4*, 94.
(9) Ishida, Y.; Yamafugi, K. *Kolloid Z. Z. Polym.* **1965**, *202*, 26.
(10) Tuijnman, C. A. F. *Polymer* **1968**, *4*, 259.
(11) Tuijnman, C. A. F. *Polymer* **1968**, *4*, 315.
(12) Stachurski, Z. H.; Ward, I. M. *J. Macromol. Sci., Phys.* **1969**, *B3*, 445.
(13) Manabe, S.; Sakado, A.; Katada, A.; Takayanagi, M. *J. Macromol. Sci., Phys.* **1970**, *B4*, 161.
(14) Kajiyama, T.; Okada, T.; Sakoda, A.; Takayanagi, M. *J. Macromol. Sci., Phy.* **1973**, *B7*, 583.
(15) Kawaguchi, T.; Ito, T.; Kawai, H.; Keedy, D. A.; Stein, R. S. *Macromolecules* **1968**, *1*, 126.
(16) Onogi, S.; Keedy, D. A.; Stein, R. S. *J. Polym. Sci.* **1961**, *50*, 153.
(17) Yamada, R.; Stein, R. S. *J. Appl. Phys.* **1965**, *36*, 3005.
(18) Takeuchi, A.; Stein, R. S. *J. Polym. Sci., Polym. Phys. Ed.* **1967**, *5*, 1079.
(19) Tanaka, A.; Chang, E.; Delf, B.; Kimura, I.; Stein, R. S. *J. Polym. Sci., Polym. Phys. Ed.* **1973**, *11*, 1891.
(20) Kyu, T.; Yasuda, N.; Suehiro, S.; Nomura, S.; Kawai, H. *Polym. J.* **1976**, *8*, 565.
(21) Suehiro, S.; Yamada, T.; Inagaki, H.; Kyu, T.; Nomura, S.; Kawai, H. *J. Polym. Sci., Polym. Phys. Ed.* **1979**, *17*, 763.
(22) Suehiro, S.; Yamada, T.; Kyu, T.; Fujita, K.; Hashimoto, T.; Kawai, H. *Polym. Eng. Sci.* **1979**, *19*, 929.
(23) Suehiro, S.; Kyu, T.; Fujita, K.; Kawai, H. *Polym. J.* **1979**, *11*, 331.
(24) Kawai, H.; Suehiro, S.; Kyu, T.; Shimomura, A. *Polym. Eng. Rev.* **1983**, *3*, 109.
(25) Matsuo, M.; Inoue, K.; Abumiya, N. *Seni Gakkaishi* **1984**, *40*, 275.
(26) Smith, P.; Lemstra, P. J. *J. Mater. Sci.* **1980**, *15*, 505.
(27) Smith, P.; Lemstra, P. J.; Booij, H. C. *J. Polym. Sci., Polym. Phys. Ed.* **1981**, *19*, 877.
(28) Sawatari, C.; Okumura, T.; Matsuo, M. *Polym. J.* **1986**, *18*, 741.
(29) Khanna, Y. P.; Turi, E. A.; Taylor, T. J.; Vickroy, V. V.; Abbott, R. F. *Macromolecules* **1985**, *18*, 1302.
(30) Matsuo, M.; Manley, R. S. J. *Macromolecules* **1982**, *15*, 985.
(31) Matsuo, M.; Manley, R. S. J. *Macromolecules* **1983**, *16*, 1500.
(32) Matsuo, M.; Tsuji, M.; Manley, R. S. J. *Macromolecules* **1983**, *16*, 1505.
(33) Matsuo, M.; Sawatari, C.; Iida, M.; Yoneda, M. *Polym. J.* **1985**, *17*, 1197.

(34) Nagamatsu, K. *Kolloid Z. Z. Polym.* **1960**, *172*, 141.
(35) Miki, K.; Hikichi, K.; Kaneko, M. *Jpn. J. Appl. Phys.* **1967**, *6*, 931.
(36) Miki, K.; Yasuda, J.; Kaneko, M. *Jpn. J. Appl. Phys.* **1969**, *8*, 159.
(37) Wada, Y.; Tsuge, K. *Jpn. J. Appl. Phys.* **1962**, *1*, 64.
(38) Okano, K. *J. Polym. Sci., Part C* **1966**, *15*, 95.
(39) Matsuo, M.; Sawatari, C., submitted for publication in *Macromolecules*.
(40) Matsuo, M.; Sawatari, C. *Macromolecules* **1986**, *19*, 2036.

Dielectric Relaxation Studies of Ion Motions in Electrolyte-Containing Perfluorosulfonate Ionomers. 1. NaOH and NaCl Systems

Kenneth A. Mauritz* and Ruey-Mei Fu

Departments of Polymer Science and Physics, University of Southern Mississippi, Southern Station Box 10076, Hattiesburg, Mississippi 39406-0076. *Received August 19, 1987*

ABSTRACT: Nafion perfluorosulfonate membranes were equilibrated in concentrated aqueous NaOH and NaCl solutions, and the dielectric response of these electrolyte-imbibed materials was investigated with an impedance analyzer. The storage and loss components of the complex dielectric constants were determined over the frequency range 5 Hz to 13 MHz as a function of external solution concentration and temperature. The observed dielectric behavior, coupled with the knowledge of polymer microphase separation, strongly suggests a mechanism of the relaxation of an interfacial polarization that arises from the accumulation and dissipation of mobile ionic charge, between electric field reversals, at the boundaries of clusters along the direction of the external applied field. Also, there is a clear manifestation of long-range ion motion that might be attributed to intercluster migration in contrast with the shorter intracluster displacements conceivably involved in the interfacial polarization process. Furthermore, it appears that the equilibrium electrolyte uptake is characterized by an exclusion of OH^- ions greater than that as predicted by simple Donnan theory even when fixed-anion aggregation is taken into account.

Introduction

Nafion[1] perfluorinated ionomers, acting mainly in the role of ion-permselective membranes, have received considerable attention over the past decade. The earliest reported investigations of structure and properties were largely driven by a competitive need to understand and control, from the standpoint of selective molecular transport, the characteristic motions of ions and water molecules within the hydration microstructure of these membranes in electrochemical cells designed for the economical production of chlorine and caustic.[2] Furthermore, the interplay between polymer microstructure, cation/anion transport selectivity, water transport, and the *electrolyte strength* of the highly concentrated salt and alkali hydroxide solutions with which these membranes interface was, and remains, an important industrial issue.

A distinguishing feature of these remarkable polymers is an underlying microstructural heterogeneity said to be characterized by ~30–50 Å wide hydrophilic *clusters*, containing fixed and free ions as well as water molecules, embedded in a hydrophobic fluorocarbon phase.[3] Fundamental models of the molecular energetics of cluster formation, and the swelling of clusters in Nafion membranes equilibrated in water, have been contributed by Hopfinger and Mauritz,[4] Hsu and Gierke,[5] and more recently Mauritz and Rogers.[6]

Regarding the hydrophobic fluorocarbon phase, the studies of Starkweather[7] indicate that the polymer chains therein are organized in a hexagonal bilayer configuration similar to the structure of poly(tetrafluoroethylene) at high temperatures.

Earlier infrared and nuclear magnetic resonance spectroscopic studies were performed by Lowry and Mauritz[8] and Komoroski and Mauritz[9a,b] on Nafion perfluorosulfonate membranes in the monovalent alkali cationic salt forms as a function of water content. These studies, by yielding important information relating to side chain–counterion interactions and internal water structure, provided an experimental foundation for a statistical mechanical four-state model of the dynamic equilibrium between bound and dissociated counterions, which, in turn, formed the backbone of a theory of membrane internal water activity[9b,c] which correctly predicted the general trend of membrane swelling with cation size.[10]

Later, Mauritz and Gray[11] determined that the electrolyte invasion of Nafion sulfonate membranes equilibrated in strong NaOH solutions is characterized by an OH^-/SO_3^- mole ratio that is quite *invariant* over the large external concentration range: $7.5 \leq M \leq 17.9$, indicating that the progressive concentration of internal NaOH, with increasing external solution concentration, is essentially a dehydration process (Figure 1). This dehydration would deswell the polymer matrix causing an increase in the fixed charge (SO_3^-) density, which in turn resists further OH^- uptake by an enhanced Donnan exclusion.

Mauritz and Gray also demonstrated how an FT-IR analysis of the O–H stretching region, for Nafion membranes equilibrated in NaOH and KOH solutions, can yield useful information that relates to (a) the underlying hydrated cluster morphology, (b) an anomalous OH^- ion mobility due to proton transfer within hydrogen bonds, and (c) Na^+–OH^- ion pairing within clusters as a function of external alkali hydroxide concentration.[11]

Nafion sulfonate membranes containing OH^- ions and varying amounts of water were seen to generate infrared spectra displaying *continuous absorption*, that is, a diffuse background-like superposition that originates at the main OH peak maximum, for the H_2O molecule, and extends continuously to lower wavenumbers. The relative degree of continuous absorption was seen to be a characteristic function of the concentration of the external aqueous alkali hydroxide solution in which the membranes were equilibrated, for a given cation type and temperature. Recognizing that the fundamental molecular event giving rise to continuous absorption is the tunneling and/or activated transfer of protons in the $H_3O_2^-$ groups throughout the

0024-9297/88/2221-1324$01.50/0